J Fluoresc (2015) 25:931–939
DOI 10.1007/s10895-015-1575-4

ORIGINAL PAPER

Evaluation of Antitumor Activity of Hesperetin-Loaded Nanoparticles Against DMBA-Induced Oral Carcinogenesis Based on Tissue Autofluorescence Spectroscopy and Multivariate Analysis

Krishnamoorthy Gurushankar[1] · Shaiju S. Nazeer[2] · Ramapurath S. Jayasree[2] · Narendran Krishnakumar[1]

Received: 28 January 2015 / Accepted: 23 April 2015 / Published online: 7 May 2015

Abstract The present study is designed to understand the nature of endogenous fluorophores and cellular metabolism that occur in the experimental oral carcinogenesis and to assess their feasibility for antitumor efficacy of hesperetin-loaded nanoparticles (HETNPs) in comparison with native hesperetin (HET) against 7,12-dimethyl benz(a) anthracene (DMBA)-induced oral carcinogenesis using fluorescence spectroscopy. The fluorescence emission spectra of the control and the experimental buccal mucosa are recorded at an excitation wavelength of 320 nm with an emission ranging from 350 to 550 nm. The results show that there is a reduced contribution from the emission of collagen, nicotinamide adenine dinucleotide (NADH) and flavin adenine dinucleotide (FAD), in DMBA-induced tumor tissues as compared with the control tissues. Furthermore, there was significant decrease in the optical redox ratio [(FAD/ (NADH+FAD)] is observed in DMBA-induced tumor tissues, which indicates an increased metabolic activity when compared to the control tissues. Oral administration of HET and its nanoparticulates restored the status of endogenous fluorophores emission and would have a higher redox ratio in the buccal mucosa of DMBA painted animals. Taken together, the treatment of nanoparticulate hesperetin was found to be more effective than native hesperetin in improving the status of endogenous fluorophores to a near normal range in DMBA-induced hamster buccal pouch carcinogenesis. The results of this study raise the important possibility that fluorescence spectroscopy in conjunction with PC-LDA has tremendous potential for monitor or potentially predict response to therapy.

Keywords Endogenous fluorophores · Oral carcinogenesis · Nanoparticluate hesperetin · Multivariate analysis

✉ Narendran Krishnakumar
nskumarphyamu@gmail.com

[1] Department of Physics, Annamalai University, Annamalainagar 608 002, Tamilnadu, India

[2] Biophotonics and Imaging Laboratory, Biomedical Technology Wing, Sree Chitra Tirunal Institute for Medical Sciences and Technology, Poojappura, Thiruvananthapuram 695 012, Kerala, India

Introduction

Oral squamous cell carcinoma (OSCC) is the sixth most common cancer worldwide with increasing incidence and mortality rate [1]. Its early detection is crucial to improve survival and reduce morbidity, disfigurement, loss of function, poor quality of life, duration of treatment and hospital costs [2, 3]. Despite numerous technological advances over the last 50 years, the survival rate linked to OSCC did not undergo a marked improvement and it amounts to approximately 50 % at 5 years [4]. Therefore, early detection of oral cancer is very important for improving 5 year survival. Unfortunately, early diagnosis has a very low rate mainly due to low rates of screening. The gold standard for oral cancer diagnosis remains tissue biopsy with histological assessment, but this technique needs a trained health-care provider, and is considered invasive, painful, expensive and time consuming [5]. As a consequence, in recent years there has been a growing and persisting demand towards developing new non-invasive, practical diagnostic tools that might facilitate the early detection of oral cancer [6]. Optical spectroscopy methods are fast emerging as potential alternatives for early diagnosis of cancer [7, 8]. A number of optical spectroscopic techniques have recently been explored as tools to improve the in vivo, real-

time detection of pre-cancers and cancers. Based on strong clinical rationale, many researchers have investigated the autofluorescence spectroscopy of tissues in the head and neck region and in various other organs, such as the bronchus, colon, cervix and esophagus for developing non-invasive screening methodologies for early diagnosis of cancer [9]. Over the last decade many reports promising for in vivo fluorescence spectroscopy can detect high-grade pre-cancer with good accuracy and also in drug monitoring. Autofluorescence of tissues is produced by fluorophores that naturally occur in living cells after excitation with a suitable wavelength [10–12]. Early pilot studies focused on UV and blue excitation wavelengths. More recently, a study of 146 patients comparing 18 different excitation wavelengths found that three broad ranges of excitation 330–340 nm (UV), 350–380 nm (UV) and 400–450 nm (blue) gave the best sensitivity and specificity for detection of high-grade pre-cancer [13]. Autofluorescence spectroscopy seeks to exploit biochemical information provided by prominent tissue fluorophores such as collagen, NADH, FAD and porphyrin [14] NADH and FAD are involved in the oxidation of metabolic molecules; therefore, direct monitoring of their fluorescence dynamically can be used to report the metabolic activity of cells and tissues [15]. Metabolic activity of the relative amounts of reduced NADH and FAD and the microenvironment of these metabolic electron carriers can be used to non-invasively monitor changes in metabolism, which is one of the hallmarks of carcinogenesis [16]. The optical "redox ratio" (fluorescence intensity of FAD divided by that sum of FAD and NADH) is widely used to monitor cellular metabolism in cells, ex vivo tissues and in vivo tissues in order to diagnose disease, monitor cellular differentiation and characterize other metabolic perturbations [16–18]. Moreover it is sensitive to early metabolic shifts after cancer treatment and has potential to non-invasively detect treatment response sooner than current methods. Hence, large-scale cell proliferation or tumor growth can be identified by significant changes in NADH and FAD fluorescence [16]. Animal models are of great importance in attempting to better understand the natural history and molecular biology of carcinogenesis. The hamster cheek pouch carcinogenesis model is a well-known and well-characterized animal model of human oral cancer and squamous cell carcinomas (SCC) [19]. Animal models of hamster buccal pouch have become an imperative tool in the development and testing of new anticancer drugs [20, 21]. Many epidemiological studies suggest that a reduced risk of cancer is associated with high consumption of vegetables and fruits. Hesperetin (HET) (3', 5, 7-trihydroxy-4-methoxyflavonone), one of the most abundant flavonoids found in citrus fruits which occurs as hesperidin (its glycoside form) in nature and it has received considerable attention in cancer prevention. It exhibits various pharmacological activities but the clinical use of hesperetin was restricted because of the poor water solubility and bioavailability. Nanomedical approaches to drug delivery center on developing nanoscale particles or molecules to improve drug bioavailability, increased water solubility and ensuring a better drug delivery system [22, 23]. Hesperetin-loaded nanoparticles (HETNPs) were synthesized by the nanoprecipitation method with their average particle size in the range of 55–180 nm and it has been described in detail previously [24]. Autofluorescence method provides a novel integrated environment in which a collection of spectral biomarkers validated on well-defined animal models may provide important clues to tumor biology and response to treatment, with potential applications in human neoplasms. Hence, the present study is designed to evaluate the antitumor efficacy of the prepared HETNPs in comparison with native HET for monitoring endogenous fluorophores emission and to quantify the metabolic changes in the redox state against DMBA-induced oral carcinogenesis by using fluorescence spectroscopic technique. Moreover, principal component and linear discriminate analysis (PC-LDA) has been used to analyze and classify the autofluorescence emission spectra acquired from the control and the experimental hamster buccal mucosa. Furthermore, receiver operating characteristic (ROC) testing is also conducted to further evaluate the performance of PC-LDA algorithms on autofluorescence spectroscopy for oral cancer diagnosis.

Materials and Methods

7,12-dimethyl benz(a) anthracene (DMBA), hesperetin (HET) and polyvinyl alcohol (PVA) (M.W. 25,000) were obtained from Sigma-Aldrich Chemical Pvt Ltd, Bangalore, India and used as received. Aminoalkyl methacrylate copolymer Eudragit® E 100 (EE 100) was a kind gift sample supplied by Evonik Industries, Mumbai, India. All other chemicals and solvents used were of analytical grade, purchased from Himedia, Mumbai, India.

Animals and Diet

The experiment was carried out with male golden Syrian hamsters aged 8–10 weeks, weighing between 100 and 110 g purchased from the National Institute of Nutrition, Hyderabad, India and were maintained in the Central Animal House, Rajah Muthiah Medical College and Hospital, Annamalai University, Tamilnadu, India. Five animals were housed in a polypropylene cage and provided with standard pellet diet (Agro Corporation Pvt. Ltd., Bangalore, India) and water ad libitum. The animals were kept under controlled conditions of temperature (27±2 °C) and humidity (55±5 %) with a light/dark cycle. The animals were maintained in accordance with the guidelines of the Indian Council of Medical Research and approved by the local

institutional animal ethical committee (Register number 160/1999/CPCSEA), Annamalai University, India.

Experimental Design

The hamsters were randomly distributed into six groups each containing 6 hamsters. Group 1 hamsters served as control and were painted with liquid paraffin alone, three times a week for 14 weeks on their left buccal pouches. The hamsters in group 2, 3 and 4 were painted with a 0.5 % solution of DMBA in liquid paraffin using a no.4 brush, three times per week for 14 weeks on their left buccal pouches [25]. Group 2 hamsters received no additional treatment. Hamsters in group 3 and 4 were orally given hesperetin at a dose of 40 mg HET/kg body weight/day and HETNPs (dose equivalent to 40 mg/kg body weight/day of HET), dissolved in 1 mL of 5 % dimethyl sulphoxide (DMSO) and dissolved in distilled water, respectively, starting 1 week before exposure to the carcinogen and continued on days alternate to DMBA painting, until the end of the experiment. Groups 5 and 6 hamsters received the same dose of HET (40 mg/kg body weight/day) and HETNPs alone (dose equivalent to 40 mg/kg body weight/day of HET) as in groups 3 and 4 throughout the experiment. The dose of HET and HETNPs used in this study were chosen based on a dose response study undertaken by us that demonstrated maximum antitumor efficacy at these dose have been reported previously [20]. The experiment was terminated at the end of 16 weeks and hamsters were sacrificed by cervical dislocation after an overnight fast. The buccal pouches were excised and the tissues were further processed for experiments. The tissue specimens from each group were frozen in liquid nitrogen and then stored at −80 °C until fluorescence spectroscopic analysis. In group 5 (HET alone) and group 6 (HETNPs alone), the epithelium was normal, intact and continuous [20]. Therefore, groups 1, 2, 3 and 4 were chosen for the further fluorescence spectroscopic analysis.

Instrumental Setup

The fluorescence spectra of left buccal pouch site of the control and the experimental hamster's tissues were measured on a Fluorolog-III spectrofluorometer (Jobin Yvon Inc., USA). The excitation light was generated from a 450 W Xenon lamp by passing through a monochromator and focused on to a 2× 6 mm spot on the surface at an angle of 45° of the sample and the fluorescence emitted from the tissues was collected at an angle of 22.5° by an emission monochromator connected to a photomultiplier tube. The excitation wavelength of 320 nm was selected using Datamax™ software (Datamax, Round Rock, Texas) and the inbuilt double-grating monochromator. Emission spectra in the range of 350 to 550 nm were recorded for 320 nm excitation.

Data Processing and Analysis

Normalizing a fluorescence spectrum removes absolute intensity information, algorithms developed from normalized fluorescence spectra rely on differences in spectral line shape information for diagnosis. When spectral shape changes are observed, they are related mainly to appearance or concentration changes in the fluorophores, which are presented in a given oral pathology, but could be as well an indicator of changes in metabolic activity of given tissue. All spectra were baseline corrected and then normalized with respect to the maximum intensity of the peak at~450 nm for the 320 nm excitation. Statistical analysis was performed for checking the variations in the prominent fluorescence peak intensity between the control and experimental buccal pouch site of the hamsters by one-way analysis of variance (ANOVA) followed by using statistical package of social science (SPSS) version 17.0 for windows.

Redox Ratio Evaluation

To accurately determine the redox ratio, the detected NADH and FAD autofluorescence intensity was considered as the measurement of cellular metabolism [16]. The reduction and oxidation ratio was computed using the relation [17].

$$\text{Redox ratio} = \left[\left(\text{FAD}_{\text{intensity}} \Big/ \left(\text{FAD}_{\text{intensity}} + \text{NADH}_{\text{intensity}}\right)\right)\right]$$

Where, FAD intensity and NADH intensity are the emission intensity at~510 and~450 nm, respectively.

Multivariate Analysis

Large dimensional spectral space (spectrum ranging from 350 to 550 nm) often results in inefficiency in execution of conventional statistical analysis. PCA is a statistical technique for simplifying complex data sets and determining the key variables in a multidimensional data set that best explain the differences in the observations [26]. In the present study, PCA on the normalized spectra of each category was performed and the data were reduced into seven principal components using statistical package of social science (SPSS) version 17.0 for windows. These principal components were used as input variables for the linear discriminant analysis (LDA) [27].

LDA classifier models were developed based on the selected variables using discriminate analysis. Data from the calibration sample set was used to develop the LDA classifier model using the full cross-validation (leave one out) option, while data from the validation sample set was used for performance evaluation of the models. The number and identity of components retained for each model therefore changes throughout the validation process. The leave one out cross validate procedure allows each combination of approaches

to be tested using data sets independent of the training samples. PCA and ANOVA were recalculated for each new training set. The classification accuracy was determined by computation of the sensitivity and specificity. In the present study LDA was performed with the statistical software package SPSS (17.0) software. The spectra of 15 from each group (1–4) were chosen from the total 60 samples to be analyzed using the PC-LDA method to extract the spectrum of each PC and its contribution to the tissue fluorescence spectra.

Receiver Operating Characteristic (ROC) Curve Analysis

The performance level of the developed classification model is further assessed by the ROC curve method. The ROC curve is a graphic method to interrogate the relationship between specificity and sensitivity under various thresholds that distinguish two populations. The false positive rates (1-specificity) as the horizontal axis versus true positive rate (sensitivity) as the vertical coordinate for Control vs DMBA, DMBA vs DMBA+HET, DMBA vs DMBA+HETNPs and DMBA+HET vs DMBA+HETNPs treated tissues under a series of different threshold values were plotted on a two dimension curve plot, as shown in Fig. 6. It can reflect the performance of a binary classifier. The concept of an ROC curve is based on the notion of a "separator" (or decision) variable. The frequencies of positive and negative results of the diagnostic test will vary if one changes the "criterion" or "cut-off" for positivity on the decision axis. In effect it enables one to establish the best possible test outcome by defining what is required of the test, i.e., no false negatives, or no missed cancers. The area under the curve of ROC can clearly show the diagnosis performance of the method. Area under the curve summarizes the ROC and provides a single measure of the performance of a classifier and the discrimination ability of the model.

Results

Spectral Features of 320 nm Excited Spectra

The average fluorescence spectral profiles in the range of 350 to 550 nm from the control and DMBA and administration of HET and HETNPs to DMBA painted hamster buccal mucosa obtained with the selected excitation at 320 nm are shown in Fig. 1. The spectrum has two main peaks at~380 nm and~450 nm and small hump~510 nm. Of these, the 380 nm peak corresponded to that of the collagen, the 450 nm peak corresponded to that of the coenzyme nicotinamide adenine dinucleotide (NADH) and the 510 nm corresponded to that of the flavin adenine dinucleotide (FAD). The major difference of the fluorescence spectral profiles of the control and the experimental buccal mucosa was found at~380 nm emission as shown in Fig. 1. It was important to note that while control

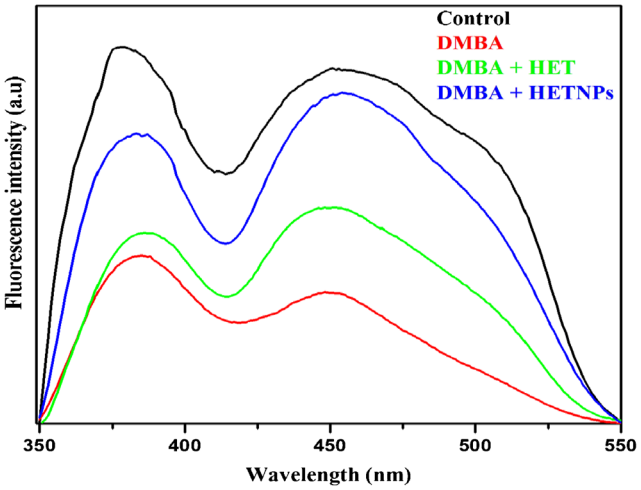

Fig. 1 Average autofluorescence spectra from the Control, DMBA-alone, DMBA+HET and DMBA+HETNPs treated tissues

tissues had the highest intensity of the~380 nm and~450 nm emission peak, followed by the DMBA+HETNPs and DMBA+HET and DMBA-induced tumor tissues. In addition, the small hump peak around 510 nm is found in the case of control, whereas in the case of tumor tissues, this peak appears as very weak. This difference indicates the change of fluorophore compositions in tissue during the tumor transformation.

Figure 2 shows the averaged normalized autofluorescence spectra of control and experimental buccal mucosa under 450 nm emission wavelength. The spectra were normalized with respect to the peak at~450 nm and hence these peaks are not considered for the analysis. The main advantage of utilizing a normalized spectrum is that fluorescence intensity does not need to be recorded in calibrated units.

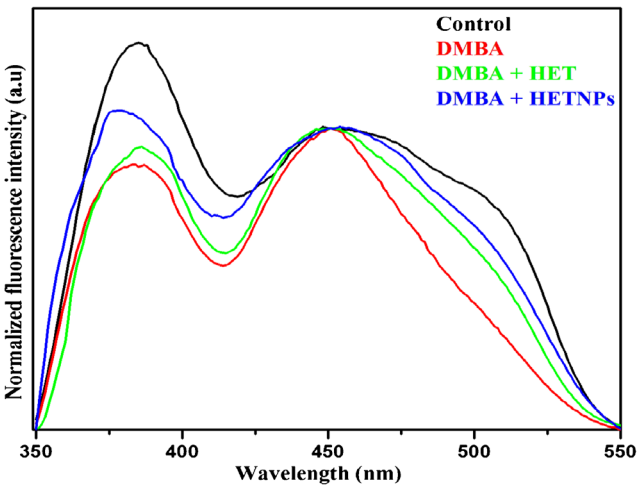

Fig. 2 Average autofluorescence spectra from normalized to the intensity at~450 nm for the Control, DMBA-alone, DMBA+HET and DMBA+HETNPs treated tissues

Optical Redox Ratio

NADH and FAD are important co-enzymes for cellular metabolism, where NADH acts as the electron donor and FAD acts as accepter in the electron transport chain of mitochondria. Relative change in such oxidation and reduction rate is termed as redox ratio. Variation in the redox ratio of the cells is used to monitor the metabolic activity level at different conditions. The increased metabolic activity and decreased blood flow due to the rapid cell division, alteration in oxygen demand and supply and genetic variation, as typically observed in cancer cells. NADH and FAD autofluorescence and the associated redox ratio, ([FAD])/([NADH]+[FAD]), have been exploited in a number of in vitro and in vivo studies for detecting changes in metabolic activity that are typically associated with neoplastic transformation [28–30]. Thus, it sought to examine the presence of differences in intensity or localization of these fluorophores between the control and the experimental tissues. The ratio values for all groups are given as a box plot and indicate clear differences between the groups are shown in Fig. 3. From this result, it is clear that there is a considerable decrease in the redox ratio for tumor tissues from that of the control tissues. On the contrary, a ratio value of redox was significantly higher in DMBA+HET and DMBA+HETNPs treated hamster buccal mucosa compared to DMBA-induced tumor tissues.

Multivariate Analysis

Multivariate data analysis can be used for inter spectral investigation where different mathematical and statistical analyses are performed to obtain pattern recognition for sample classification. To understand the changes of relative contents of principle biochemical components in the cancerous and normal tissues, the spectrum of each component and its weighted contribution to the entire tissue fluorescence spectra were extracted from the measured fluorescence spectra of the cancerous and normal tissues using the PC-LDA method. Since the current study aims to discriminate between the control and the experimental groups, the discriminant analysis was performed across four groups, (i.e.,) Control, DMBA, DMBA+HET and DMBA+HETNPs treated hamster buccal pouch tissues resulted in the canonical discriminant function. Canonical discriminant analysis was performed between the control and the experimental buccal mucosa of hamsters. The same ratio parameters were incorporated into the function. A visual approach to interpreting the dicriminant functions is to plot each group centroid in a two dimensional plot with one function against another function. Figure 4 shows the two dimensional plot between discriminant function I and discriminant function II. Function 1 separates the groups as far as possible. Function II is uncorrelated with function I and further separates the groups, the result of which allows for the maximum separation between groups and minimal separation within groups. The discriminant scores of each dependent variable for the four study groups are separated. Pairwise discriminant function scatter plots for the control, DMBA, DMBA+HET and DMBA+HETNPs treated tissues generated by PC-LDA at 320 nm excitation spectra are given in Fig. 5. Discrimination line drawn at 0 gives a good separation for the control and the experimental groups. The sensitivity and specificity indices of the diagnostic algorithm were calculated using pairwise correlation of LDA score with the determined cut off values given in Fig. 5. Using the position of pairwise discrimination scores, the number of true positive and negative values as well as the number of false positive

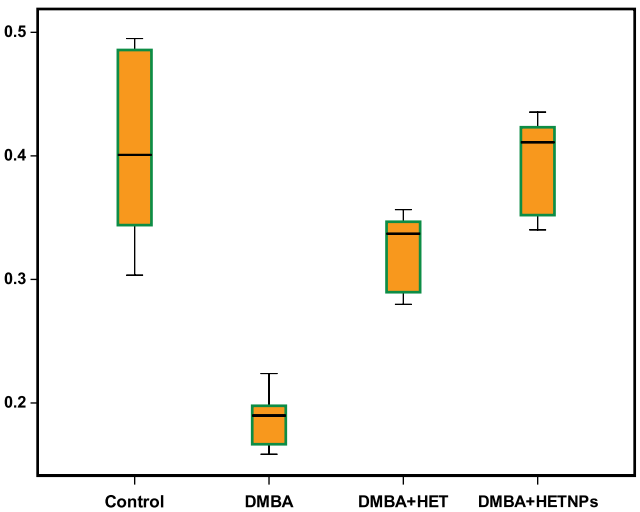

Fig. 3 Optical redox ratio [Autofluorescence intensity of FAD/(NADH+FAD)] for the Control, DMBA-alone, DMBA+HET and DMBA+HETNPs treated tissues

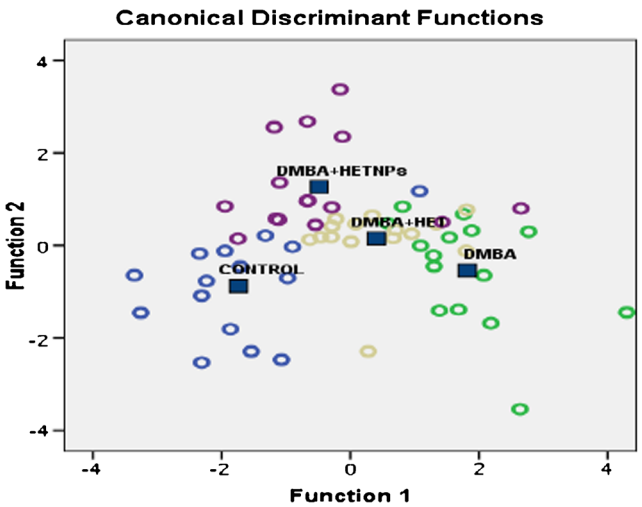

Fig. 4 Canonical discriminant of the function 1 and function 2 discriminance values for each lesion are plotted. Control (CON): *blue circles*, DMBA: *green circles*, DMBA+HET: *light yellow circles* and DMBA+HETNPs: *thick blue circles*. The center of each cluster is marked by an *open square* in the appropriate color

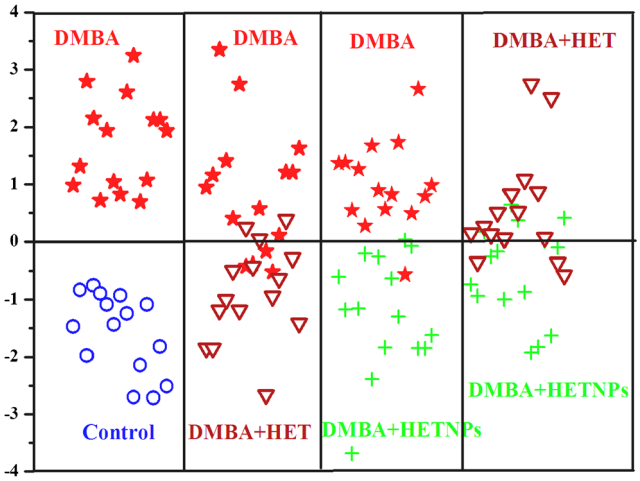

Fig. 5 Pairwise discriminant function scatter plot of different group pairs of Control vs DMBA, DMBA vs DMBA+HET, DMBA vs DMBA+HETNPs and DMBA+HET vs DMBA+HETNPs treated tissues

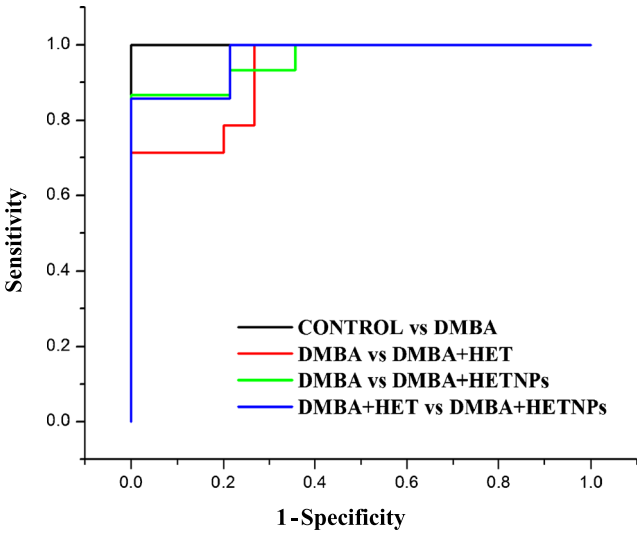

Fig. 6 The receiver operator characteristic (ROC) curves showing the diagnostic performance of discriminant scores of Control vs DMBA (AUC=1.00), DMBA vs DMBA+HET (AUC=0.84), DMBA vs DMBA+HETNPs (AUC=0.97) and DMBA+HET vs DMBA+HETNPs (AUC=0.96) treated tissues

and negative values was obtained. The diagnostic performance of fluorescence spectroscopic evaluation is distinctively evaluated using binary calculation results, sensitivity (Se), specificity (Sp), accuracy, positive predictive value (PPV) and negative predictive value (NPV). PPV gives the probability of disease if a test result is positive, while NPV gives the probability of no disease if a test result is negative. Those parameters are defined as Se=TP/ (TP+FN), Sp=TN/ (TN+FP), Accuracy=TP+TN/ (P+N), PPV=TP/(TP+FP) and NPV= TN/(FN+TN), where TP, FP, TN, and FN are the numbers of true positives, false positives, true negatives and false negatives, respectively. Results from this binary classification are utilized for the discrimination of tissues (Table 1). The sensitivity and specificity of Control vs DMBA, DMBA vs DMBA+HET, DMBA vs DMBA+HETNPs and DMBA vs DMBA+HETNPs groups were found to be 100, 66.67, 86.67 and 73.3 % and 100, 71.42, 80.0 and 78.57 %, respectively. In addition, a comparative evaluation of the ROC curves (Fig. 6) indicates that PC-LDA based diagnostic algorithm gives more effective diagnostic performances for differentiation of the control and the experimental groups. The area under the curve of ROC can clearly show the diagnosis performance of the method. The areas under the ROC curve for Control vs DMBA, DMBA vs DMBA+HET, DMBA vs HETNPs and DMBA+HET vs DMBA+HETNPs tissues were 1.00, 0.84, 0.97 and 0.96, respectively.

Discussion

Recent research has shown that fluorescence spectroscopy has the capability to quickly, non-invasively and quantitatively probe the biochemical and morphological changes that occur as tissue becomes neoplastic. An alteration in the oral mucosa produce alterations at cellular level and also changes in structural tissue composition, which in turn will have an effect on the spectral shape and intensity, the analysis of which can provide information that may contribute to diagnosis. Metabolic disturbances in cells can be reflected in the tissues themselves or in body fluids and cause changes in fluorophore concentrations. Several studies in the literature cite the importance of native fluorescence spectroscopy using intrinsic fluorophores as metabolic indicators.

Collagen is the most abundant protein in the human body. Due to internal and external factors, collagen undergoes a variety of modifications resulting in serious diseases. In this study, as observed by the peak intensity around 380 nm under this peak, a decrease in the collagen level is observed for DMBA, DMBA+HET and DMBA+HETNPs tissues when compared with control tissues [Figs. 1 and 2]. The decrease in collagen can be attributed to the degradation of extracellular

Table 1 Classification efficiency classified using PC-LDA for the differentiation of the control and the experimental tissues

Groups	Sensitivity (%)	Specificity (%)	Accuracy (%)	PPV (%)	NPV (%)
Control vs DMBA	100	100	100	100	100
DMBA vs DMBA+HET	66.6	71.4	72.5	73.3	68.7
DMBA vs DMBA+HETNPs	86.6	80.0	83.3	81.2	85.7
DMBA+HET vs DMBA+HETNPs	73.3	78.5	80.0	76.4	84.6

matrix that takes place to facilitate the migration of neoplastic cells to the surrounding tissues during the tumor cell invasion process. Moreover, decrease in penetration of excitation light through thickened epithelial layer and loss of signal of collagen from below basement membrane as well as collagen lysing. It has also been shown that collagenase enzymes responsible for the degradation of collagen are usually present in tissue areas undergoing significant architectural changes, resulting in the observed changes in NADH and collagen contributions to the tissue fluorescence spectrum with progression of disease [31]. Lane et al. [32] attribute the loss of autofluorescence signal in images of oral precancerous and cancerous lesions primarily to the breakdown of the collagen matrix and increased hemoglobin absorption and secondarily to epithelial factors, such as increased epithelial scattering and thickness. Further, Drezek et al. [33] reported that matrix metalloproteinases released from epithelial cells may break down the collagen crosslinks causing the collagen matrix to appear less fluorescent in dysplastic samples. The increased thickness of the tumor tissues thus led to the decrease of the collagen (~380 nm) and NADH (~450 nm) signals by filtering the autofluorescence from deeper tissue layers. In the present study, NADH as well as FAD fluorescence intensities are reduced significantly observed for DMBA, DMBA+HET and DMBA+HETNPs tissues when compared with the control tissues. This change could be the result of an increased number of cells and/or increased levels of metabolic activity in the tissues. Redox ratio has been used effectively as an indicator of metabolic activity as well for yielding more reliable information than measuring either NADH or FAD fluorescence intensity alone. Skala et al. [16] have reported a considerable difference in redox ratio values with respect to the level of malignancy using fluorescence lifetime studies in ex vivo and in vitro conditions. In the present study, it was found that the redox ratio of DMBA-induced tumor tissues is significantly lower compared to that of control tissues and the level of this decrease was higher than the level of changes it detected in each of the fluorophores individually [Fig. 3]. This decrease in the redox ratio corresponds to an increase in metabolic activity associated with DMBA-induced tumor transformation, which is consistent with increased proliferation of cancerous cells mediated by the action of the DMBA. On the other hand, a ratio value of redox was significantly higher in DMBA+HET and DMBA+HETNPs treated hamster buccal mucosa compared to DMBA-induced tumor tissues. Entertainingly, treatment of hamsters with DMBA+HETNPs resulted in increased redox ratio value compared to those from any other DMBA-administrated animals, indicating a decrease in metabolic activity. Recent studies reported that nanoparticulate drug delivery systems exhibited more efficient anti-tumor efficacy and minimize systemic toxicity [34]. The size of resulting HETNPs was measured by using dynamic light scattering (DLS) particle analysis as well as transmission electron microscopy (TEM) and reported in detail in our previous paper [24]. According to the results of the previous study, the average particle size of HETNPs obtained in the range of 55–180 nm. Diameter of nanoparticles less than 200 nm are known to have advantages for drug targeting because this size could increase blood circulation by avoiding reticuloendothelial system (RES) and then increase chance to access the microvessel of the tumor tissue. This tumor targeting effect is ubiquitously adapted in antitumor therapy. Accordingly, it was suggested that HETNPs might facilitate the delivery of antitumor drugs into the tumor with long-term retention in the tumor, which would enhance the superior antitumor effect and also the changes in the redox state compared to native HET. Multivariate statistical analysis was also implemented for classification between control and the tumor tissues. Here, all spectra were analyzed by PCA and LDA. To test for the predictive value of fluorescence spectra PCA followed by LDA was employed in distinguishing the control and the tumor tissues. The criteria also implemented that were used to measure the quality of binary (two-class) classification as sensitivity, specificity and accuracy into this research. Sensitivity and specificity reflect the method in the aspects of identifying positive and negative results, respectively. In this study, sensitivity and specificity of Control vs DMBA, DMBA vs DMBA+HET, DMBA vs DMBA+HETNPs and DMBA+HET vs DMBA+HETNPs are 100, 66.6, 86.6 and 73.3 % and 100, 71.4, 80.0 and 78.5 %, respectively, for 320 nm excited spectra using PC-LDA is achieved for the differentiation of the control and the experimental groups. ROC analysis showed that PCA, followed by LDA, could differentiate between Control vs DMBA, DMBA vs DMBA+HET, DMBA vs DMBA+HETNPs and DMBA+HET vs DMBA+HETNPs treated tissues (Fig. 6). From this Figure it is evident that both the ROC curves are very close to the point of ideal performance (i.e., the upper left hand corner) thus indicating that both the diagnostic algorithms are reasonably accurate. One of the most popular measures of the accuracy of a diagnostic test is the area under the ROC curve. In the current study, the accuracy was considered excellent when the area under the curve was greater than 0.8 (Fig. 6). This further demonstrates that PC-LDA-based diagnostic algorithms can be used for the discrimination of control and experimental groups with good performance. The present results further demonstrating that fluorescence spectra in conjunction with a multivariate statistical analysis can be used as a potential tool for the discrimination of control and experimental groups with improved classification accuracy.

Conclusion

In conclusion, the present study has shown that fluorescence spectroscopy can be used to evaluate the antitumor efficacy of

the prepared HETNPs in comparison with native HET for monitoring endogenous fluorophores emission and to quantify the metabolic changes in the redox state against DMBA-induced oral carcinogenesis. The results show that there is a reduced contribution from the emission of collagen, NADH and FAD in DMBA-induced tumor tissues as compared with the control tissues. Furthermore, there was significant decrease in the optical redox ratio is observed in DMBA-induced tumor tissues, which indicates an increased metabolic activity when compared to the control tissues. Oral administration of HET and its nanoparticulates restored the status of endogenous fluorophores emission and would have a higher redox ratio in the buccal mucosa of DMBA painted animals. Overall, the treatment of nanoparticulate hesperetin was found to be more effective than native hesperetin in improving the status of endogenous fluorophores to a near normal range in DMBA-induced hamster buccal pouch carcinogenesis. The results of this study raise the important possibility that fluorescence spectroscopy in conjunction with PC-LDA has tremendous potential for monitor or potentially predict response to therapy.

Acknowledgments The authors are thankful to the authority of Annamalai University for providing all necessary facilities to carry out the present study.

References

1. Gillison ML (2007) Current topics in the epidemiology of oral cavity and oropharyngeal cancers. Head Neck 29:779–792
2. Scott S, McGurk M, Grunfeld E (2008) Patient delay for potentially malignant oral symptoms. Eur J Oral Sci 116:141–147
3. Rogers SN, Brown JS, Woolgar JA, Lowe D, Magennis P, Shaw RJ, Sutton D, Errington D, Vaughan D (2009) Survival following primary surgery for oral cancer. Oral Oncol 45:201–211
4. Hayat MJ, Howlader N, Reichman ME, Edwards BK (2007) Cancer statistics, trends, and multiple primary cancer analyses from the surveillance, epidemiology, and end results (SEER) program. Oncologist 12:20–37
5. Nair D, Pruthy P, Pawar U, Chaturvedi P (2012) Oral cancer: premalignant conditions and screening-an update. J Cancer Res Ther 8:s57–s66
6. Mercadante V, Paderni C, Campisi G (2012) Novel non-invasive adjunctive techniques for early oral cancer diagnosis and oral lesions examination. Curr Pharm Des 18:5442–5451
7. Swinson B, Jerjes W, El-Maaytah M, Norris P, Hopper C (2006) Optical techniques in diagnosis of head and neck malignancy. Oral Oncol 42:221–228
8. Liu Q (2011) Role of optical spectroscopy using endogenous contrasts in clinical cancer diagnosis. World J Clin Oncol 2:50–63
9. Liu W, Zhang XH, Liu KP, Zhang SD, Duan YX (2013) Laser-induced fluorescence: progress and prospective for *in vivo* cancer diagnosis. Chin Sci Bull 58:2003–2016
10. De Veld DCG, Witjes MJH, Sterenborg HJCM, Roodenburg JLN (2005) The status ofin vivo autofluorescence spectroscopy and imaging for oral oncology. Oral Oncol 41:117–131
11. Li BH, Xie SS (2005) Autofluorescence excitation-emission matrices for diagnosis of colonic cancer. World J Gastroenterol 11: 3931–3934
12. Zhang L, Pu Y, Xue J, Pratavieira S, Xu B, Achilefu S, Alfano RR (2014) Tryptophan as the fingerprint for distinguishing aggressiveness among breast cancer cell lines using native fluorescence spectroscopy. J Biomed Opt 19:037005
13. Chang SK, Follen M, Malpica A, Utzinger U, Staerkel G, Cox D, Atkinson EN, MacAulay C, Richards-Kortum R (2002) Optimal excitation wavelengths for discrimination of cervical neoplasia. IEEE Trans Biomed Eng 49:1102–1111
14. Sulfikkarali NK, Krishnakumar N (2013) Evaluation of the chemopreventive response of naringenin-loaded nanoparticles in experimental oral carcinogenesis using laser-induced autofluorescence spectroscopy. Laser Phys 23:045601
15. Rajaram N, Reichenberg JS, Migden MR, Nguyen TH, Tunnell JW (2010) Pilot clinical study for quantitative spectral diagnosis of non-melanoma skin cancer. Lasers Surg Med 42:716–727
16. Skala MC, Riching KM, Bird DK, Fitzpatrick AG, Eickhoff J, Eliceiri KW, Keely PJ, Ramanujam N (2007) *In vivo* multiphoton fluorescence lifetime imaging of protein-bound and free nicotinamide adenine dinucleotide in normal and precancerous epithelia. J Biomed Opt 12:024014
17. Ostrander JH, McMahon CM, Lem S, Millon SR, Brown JQ, Seewaldt VL, Ramanujam N (2010) Optical redox ratio differentiates breast cancer cell lines based on estrogen receptor status. Cancer Res 70:4759–4766
18. Shah AT, Beckler MD, Walsh AJ, Jones WP, Pohlmann PR, Skala MC (2014) Optical metabolic imaging of treatment response in human head and neck squamous cell carcinoma. PLoS ONE 9:e90746
19. Nagini S, Letchoumy PV, Thangavelu A, Ramachandran CR (2009) Of humans and hamsters: a comparative evaluation of carcinogen activation, DNA damage, cell proliferation, apoptosis, invasion, and angiogenesis in oral cancer patients and hamster buccal pouch carcinomas. Oral Oncol 45:e31–e37
20. Gurushankar K, Nazeer SS, Gohulkumar M, Jayasree RS, Nirmal MR, Krishnakumar N (2014) Endogenous porphyrin fluorescence as a biomarker for monitoring the anti-angiogenic effect in antitumor response to hesperetin loaded nanoparticles in experimental oral carcinogenesis. RSC Adv 4:46896–46906
21. Krishnakumar N, Sulfikkarali NK, Manoharan S, Venkatachalam P (2013) Raman spectroscopic investigation of the chemopreventive response of naringenin and its nanoparticles in DMBA-induced oral carcinogenesis. Spectrochim Acta A 115:648–653
22. Krishnakumar N, Sulfikkarali NK, Rajendra Prasad N, Karthikeyan S (2011) Enhanced anticancer activity of naringenin-loaded nanoparticles in human cervical (HeLa) cancer cells. BioMed Prev Nutr 1:223–231
23. Gohulkumar M, Gurushankar K, Rajendra Prasad N, Krishnakumar N (2014) Enhanced cytotoxicity and apoptosis-induced anticancer effect of silibinin-loaded nanoparticles in oral carcinoma (KB) cells. Mater Sci Eng C 41:274–282
24. Gurushankar K, Gohulkumar M, Rajendra Prasad N, Krishnakumar N (2014) Synthesis, characterization and *in vitro* anti-cancer evaluation of hesperetin-loaded nanoparticles in human oral carcinoma (KB) cells. Adv Nat Sci Nanosci Nanotechnol 5:015006
25. Shklar G (1999) Development of experimental oral carcinogenesis and its impact on current oral cancer research. J Dent Res 78: 1768–1772
26. Bergholt MS, Zheng W, Lin K, Ho KY, Teh M, Yeoh KG, So JB, Huang Z (2011) Combining near-infrared-excited autofluorescence and Raman spectroscopy improves *in vivo* diagnosis of gastric cancer. Biosens Bioelectron 26:4104–4110
27. Nazeer SS, Saraswathy A, Gupta A, Jayasree RS (2014) Fluorescence spectroscopy to discriminate neoplastic human brain

lesions: a study using the spectral intensity ratio and multivariate linear discriminant analysis. Laser Phys 24:025602
28. Georgakoudi I, Jacobson BC, Müller MG, Badizadegan K, Carr-Locke DL, Sheets EE, Crum CP, Dasari RR, Van Dam J, Feld MS (2002) NAD(P)H and collagen as *in vivo* quantitative biomarkers of epithelial pre-cancerous changes. Cancer Res 62:682–687
29. Pavlova I, Sokolov K, Drezek R, Malpica A, Follen M, Richards-Kortum R (2003) Microanatomical and biochemical origins of normal and precancerous cervical autofluorescence using laser-scanning fluorescence confocal microscopy. Photochem Photobiol 77:550–555
30. Levitt J, Baldwin A, Papadakis A, Puri S, Xylas J, Münger K, Georgakoudi I (2006) Intrinsic fluorescence and redox changes associated with apoptosis of primary human epithelial cells. J Biomed Opt 11:064012
31. Badizadegan K, Backman V, Boone CW, Crum CP, Dasari RR, Georgakoudi I et al (2004) Spectroscopic diagnosis and imaging of invisible pre-cancer. Faraday Discuss 126:265–279
32. Lane PM, Gilhuly T, Whitehead P et al (2006) Simple device for the direct visualization of oral-cavity tissue fluorescence. J Biomed Opt 11:024006
33. Drezek R, Brookner C, Pavlova I, Boiko I, Malpica A, Lotan R, Follen M, Richards-Kortum R (2001) Autofluorescence microscopy of fresh cervical-tissue sections reveals alterations in tissue biochemistry with dysplasia. Photochem Photobiol 73:636–641
34. Jain AK, Swarnakar NK, Das M, Godugu C, Singh RP, Rao PR, Jain S (2011) Augmented anticancer efficacy of doxorubicin-loaded polymeric nanoparticles after oral administration in a breast cancer induced animal model. Mol Pharm 8:1140–1151